PROCEEDINGS, 49th Workshop on Geothermal Reservoir Engineering
Stanford University, Stanford, California, February 12-14, 2024
SGP-TR-227

Aluminum-Rich Cements for High Temperature Geothermal Wells

Tatiana Pyatina[1], Toshifumi Sugama[1]

[1]Brookhaven National Laboratory

734 Brookhaven Ave. Upton, NY 11973

tpyatina@bnl.gov

Keywords: geothermal cement, supercritical cement; cement CO_2 exposure; metal-cement corrosion protection; OPC degradation in supercritical CO_2.

ABSTRACT

This paper presents results of design and evaluations of various Al-rich cements under supercritical hydrothermal and CO_2 field conditions. Results of short-to-longterm exposure tests up to 30 days under hydrothermal and up to 9 months under supercritical CO_2 environments are reported including mechanical properties, morphological, and phase changes for calcium-aluminate cement-based blends. Performance of aluminum-rich cement formulations is compared to that of Ordinary Portland Cement (OPC) with silica blend. The results confirm that properties of the blends with lower calcium content persist under supercritical CO_2, while the OPC blend undergoes severe degradation with the loss of mechanical properties. For alkali activated and chemical blends partial carbonation occurs through calcium carbonation. Electrochemical corrosion tests showed that Al-rich cement formulations can provide Ni-alloy corrosion protection under supercritical conditions. All tested calcium-aluminate-cement based blends outperformed OPC/silica under the CO_2-rich well conditions.

1. INTRODUCTION

Geothermal wells are constructed similarly to oil and gas ones. However, because of the high thermo-mechanical stresses they are cemented throughout to avoid casing buckling and damage. Although cement formulations similar to oil and gas wells are routinely used for geothermal well cementing, the conditions that they have to withstand may differ significantly. These include chemically aggressive environments with high well temperatures and repeated thermal and mechanical shocks. Because of the formations fragility of many economic geothermal reservoirs, lightweight Ordinary Portland cement (OPC) – based designs are often used for well construction. Decomposition of Portland-cement under geothermal conditions is accelerated by the high-temperature (HT) acidic environments and lower durability of lightweight cement compared against formulations of regular density. Commonly encountered acidic gases of geothermal wells are geological carbon dioxide and hydrogen sulfide.

Although extensive, oil and gas cementing experience has limitations in geothermal applications because of the difference in well environments, temperatures, and durability expectations. Another well-construction field that can offer potentially useful information for geothermal well cementing is underground carbon storage. Under hydrothermal environments of underground formations CO_2 creates mild acid that degrades OPC-based cement. However, the majority of underground wells considered or used for CO_2 storage are shallow with relatively low temperatures and, as a result, slow cement degradation reaction kinetics. Most previous laboratory and field studies demonstrated slow OPC degradation rate at low temperatures and/or low humidity conditions (Crow et al., 2009; Garnier et al., 2014; Kuip van der et al., 2011; Sminchack et al., 2014; Sminchak et al., 2014). Considering that the economic geothermal wells are those at HT in permeable (or stimulated) formations favorable for migration of geological gases, significantly accelerated cement degradation kinetics can be expected.

Higher temperature wells are very attractive because they can provide more energy. There is a growing interest in building and producing supercritical geothermal wells (Asanuma et al., 2012, 2015; Friðleifsson & Elders, 2005; Garrison et al., 2020; Muraoka et al., 2014; Reinsch et al., 2017). However, only very limited information is available on cementitious materials performance under supercritical conditions (Pyatina & Sugama, 2023a; Sakuma et al., 2021; Sugama & Pyatina, 2022).

In this paper we report results of evaluation of several calcium-aluminate cement-based formulations after exposure in a HT geothermal well (350°C) for 9 months and after exposure to supercritical conditions for 30 days in a laboratory setting. Performance of these formulations and of the control, OPC/Silica blend, under these two different environments that can be expected in very hot geothermal well is compared.

2. MATERIALS AND METHODS

Calcium aluminate cements (CAC), Secar #80-, Secar #71-, and Class G OPC, were used in this study. All CACs were supplied by Imerys, while Lafarge, North America provided OPC, Class G, well cement. The X-ray powder diffraction (XRD) data showed that the crystalline compounds of #80 CAC were the following three principal phases, calcium monoaluminate ($CaO.Al_2O_3$, CA), calcium dialuminate ($CaO.2Al_2O_3$, CA_2) and corundum (α-Al_2O_3). The Class G consisted of hatrurite ($3CaO.SiO_2$) as a major, and brownmillerite ($4CaO.Al_2O_3.Fe_2O_3$), basanite ($CaSO_4.1/2H_2O$) and periclase (MgO) as minor phases for the former cement. Among the cement-forming constituents, SMS (Na_2SiO_3), alkali-activating powder, of 93% purity, with the particles' size of 0.23- to 0.85-mm, trade named

"MetsoBeads 2048," was supplied by the PQ Corporation. It had a 50.5/46.6 Na_2O/SiO_2 weight ratio. Sodium hexa-meta-phosphate (SHMP) [$(NaPO_3)_6$, 60-70% P_2O_5] with 200 mesh granular obtained from Sigma-Aldrich was used as a cement-building component of calcium-phosphate cements. Silica flour was supplied by Cudd Energy Services. The metakaolin ($Al_4Si_2O_{10}$), was obtained from Imerys. FAF was supplied by Boral Material Technologies. The XRD analysis of FAF showed that it included three major crystalline phases, quartz (SiO_2), mullite ($3Al_2O_3.2SiO_2$), and hematite (Fe_2O_3).

All formulations exposed in Newberry well for 9 months were modified with 5% by weight of dry blend carbon microfibers (CMF, AGM-94) derived from a polyacrylonitrile precursor, supplied by Asbury Graphite Mills, Inc. They were 7-9 microns in diameter and 100-200 microns in length. These fibers are stable at temperatures up to 600°C. They were used to improve mechanical properties of the tested composites.

Formulations of cement samples tested in Newberry well are given in Table 1. The dry blends were prepared by shaking all the dry components for 3 minutes by hand. Water was then added to dry blends at the amount that allowed the slurries to have equal self-leveling. The slurries were placed into molds (20x40 mm) and left at room temperature for 12 hours. Then samples were demolded and exposed to 85°C environment with relative humidity of 99.9% for another 12 hours. Finally, they were autoclaved at 300°C for 12 more hours in non-stirred Parr Reactor 4622, before the shipment to the wellsite for the exposure.

All the blends for the supercritical tests were prepared in a similar manner. They were dry-mixed before adding water; the slurries were hand-mixed until getting a uniform suspension for about 2 minutes, then poured into 20x40 mm cylindrical molds, left at room temperature overnight, then cured under hydrothermal conditions at 85°C (overnight) followed by overnight hydrothermal curing at 300°C and the final curing under the supercritical (*sc*) conditions at 400°C and pressure of 25.5 MPa in Parr autoclave reactor rated for temperatures up to 500°C and pressures of 34.46 MPa (5,000 psi). Inconel steel rapture disk rated to that pressure was used for the reported formulations. The autoclave was modified to avoid rapid corrosion of the rapture disk under the supercritical conditions (Sugama & Pyatina, 2022).

Ni alloy plates (625 Nickel sheets) were used to evaluate composite-metal bond under supercritical conditions. The alloy was selected based on the recommendations of the Icelandic research team (Kaldal et al., 2015). The plates were purchased from McMaster-carr. To perform the tests plates were connected by a thin cement layer and left under weight of 20g overnight. Then they were cured in the same sequence as bulk composite samples.

Table 1. Cement formulations used in this study.

Formulation	Composition (wt. %, activator % by weight of cement blend)
CSH-60/40	OPC/SiO_2 (60/40)
TSRC	CAC#80/FAF/SMS (60/40, SMS at 6%)
CAP#71/Silica	CAC#71/Silica/SHMP (70/30, SHMP at 6%)
CAP#71/FAF	CAC#71/FAF/SHMP (70/30, SHMP at 6%)
CAP#71/Silica/MK	CAC#71/FAF/MK/SHMP (60/30/10, SHMP at 6%)
#80/Silica	CAC#80/SiO_2 (60/40)

Information on exposure tools and well conditions can be found in (Pyatina et al., 2023).

The uniaxial compressive strength, Young's modulus, and compressive toughness were determined using Electromechanical Instron System Model 5967. The measurements were done on unconfined dry samples. The instrument had a 30 kN load capacity, and the measurements were performed at a 1.25 cm/min loading rate. The compressive toughness was computed from the area under the compressive stress-strain curve.

Lap-shear bond strength at Ni alloy plate /composite adhesive/Ni alloy plate joint was measured using Electrochemical Instron System. Plates bonded by a thin layer of a composite were exposed to supercritical conditions for 7 or 30 days before the testing. After the lap-shear bond tests the plate with the thinner cement layer was used to determine the corrosion rate of the alloy. To obtain information on the protection of the metal by composites against brine-caused corrosion, DC electrochemical testing for the underlying Ni alloy was performed using the Princeton Applied Research Model Versa STAT 4 Corrosion Measurement System. In this assessment, the metal plates used in the lap-shear bond tests, with composite-adhered their surface, were mounted into a holder, and then inserted into the Ametex Model K0235 flat cell containing a 1.0 M sodium chloride electrolyte solution. The test was conducted under an aerated condition at 25°C, on an exposed surface area of 1.0 cm^2. The polarization curves were measured at a scan rate of 0.17 mVs^{-1} in the corrosion potential range from -0.4 to +0.6 V. The average corrosion rate, mm/year (mmpy), associated with the corrosion potential, $E_{corr.}$, mV, and corrosion current density, $I_{corr.}$, µA, was obtained by averaging Tafel fit results of the polarization curves of three samples.

3. RESULTS AND DISCUSSION

3.1 Mechanical Properties and Porosity Changes

Figure 1 shows UCS (Unconfined Compressive Strength) of samples exposed to supercritical conditions and to Newberry well environment for 9 months. As mentioned above the samples that were exposed in Newberry well were modified with 5% CMF. This resulted in higher strength after the 1-day curing at 300°C than for non-modified samples later exposed to supercritical conditions. Although the trend of the strength changes after the 30-day supercritical curing and 9-month well exposure was similar for the reported formulations, the magnitude of the change differed dramatically. When compared to the strength developed after the first day of curing at 300°C three formulations increased in strength and two decreased after the 30-day supercritical curing and the 9-month well exposure. The strength of #80/Silica and TSRC increased both after the supercritical 30-day and Newberry well 9-month exposures. The strength increase was 24 and 59% respectively for these two formulations under supercritical conditions; the strength more than doubled (130 and 124% increase respectively) after the 9 months in the well. In the case of calcium phosphate cement an initial strength decrease is generally expected before the strength stabilization. This trend was observed for the supercritical samples where the strength decreased consecutively after 1 and 7 days of curing but increased after the 30-day exposure. The strength increase was moderate and comparable to that under the conditions of Newberry well (5 and 8% respectively). That formulation had a very high strength of more than 30 MPa already after the first day of autoclaving at 300°C. As a result, even with the small strength increase, it remained the one with the highest strength among the tested designs.

The two designs that experienced strength decrease were that of calcium phosphate cement modified with metakaolin and the reference OPC/Silica blend. The strength of metakaolin-modified phosphate cement increased through the first 7 days of supercritical curing, however after the 30-day exposure the blend lost 57% of its original strength. The strength loss was only 10% for the field exposed samples. For the reference blend there was dramatic difference in behavior under supercritical and well conditions. The blend lost about 13% of its strength after the 30 days under supercritical conditions but 86% after the 9 months in the well. The final strength of the field-exposed samples was ~5 MPa, which is below the required 7 MPa limit for geothermal cements.

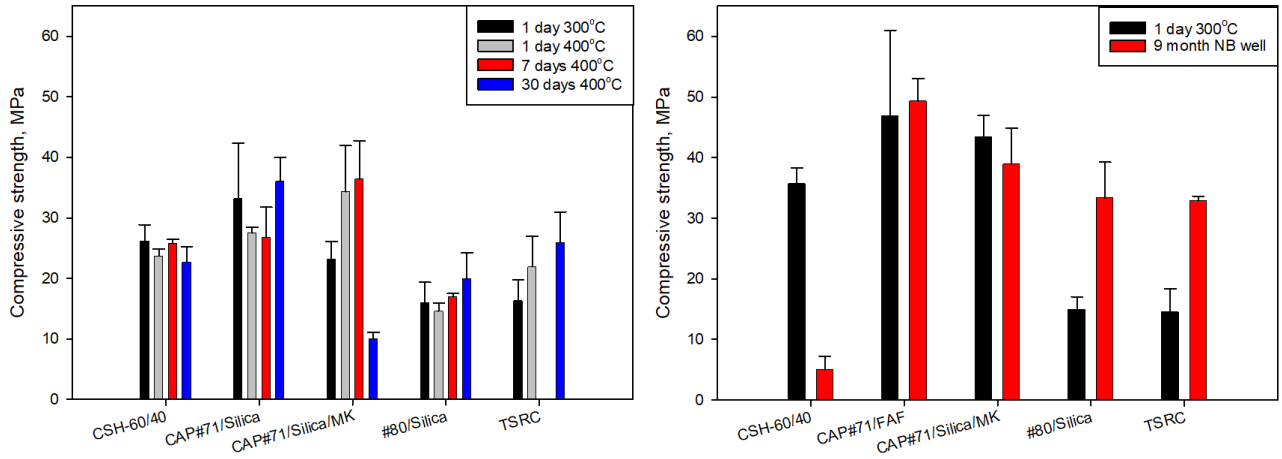

Figure 1: Unconfined compressive strength of tested composites after 1-day 300°C autoclaving, supercritical curing, and 9 months of the Newberry well exposure.

The Young's moduli for these formulations are shown in Figure 2. The YM generally mirrors compressive strength. The one exception to that was the formulation with calcium phosphate cement (both with silica and FAF). Although tis strength increased both after the supercritical curing and the Newberry well exposure, its YM decreased by 4% after the 30 days at 400°C and by 13% after the 9 months in Newberry well. For the rest of the samples the changes in YM followed those in compressive strength, increasing for #80/Silica and TSRC (by 6 and 45% respectively after the supercritical curing and by 85 and 87% after the 9-month exposure) and decreasing for OPC/Silica (CSH-60/40, by 4% after the supercritical curing and, dramatically, by 76% after the 9-month exposure). Earlier we proposed using YM to classify cement failure mode from soft (YM < 0.7 GPa) to moderate (YM: 0.7 GPa - 2 GPa), brittle (YM: 2 GPa - 3.4 GPa) and very brittle (YM > 3.4 GPa) (Pyatina & Sugama, 2020). Based on this classification calcium phosphate cement has very brittle failure both after supercritical curing and well exposure tests despite a slight decrease in YM compared to 1-day 300°C cured samples of these cement. For the samples cured under supercritical conditions, #80/Silica and TSRC had moderate failure mode before the curing and were borderline brittle after the 30 days of curing. CAP#71/Silica/MK Decreased in YM and shifted from borderline brittle failure to the moderate failure mode, the CSH-60/40 showed brittle failure after a day at 300°C and 30 days of 400°C curing.

The samples prepared for the 9-month exposure tests originally had lower YM values because of the CMF. CSH-60/40, #80/Silica, and TSRC had desirable moderate failure mode after a day at 300°C curing. The 9-month exposure shifted the failure into the brittle region for #80/Silica and TSRC, while the strength loss of the OPC formulation resulted in soft failure, with the samples crumbling under a small pressure (YM = 0.43 GPa).

In short, for most samples that withstood the exposure conditions the YM increased, and ductility decreased. The difference in the resulting YM values was not significant for the 30-day supercritical and 9-month well exposures despite significant difference in the exposure time. This is likely due to the enhanced ductility effect of CMF used in the 9-month exposed samples.

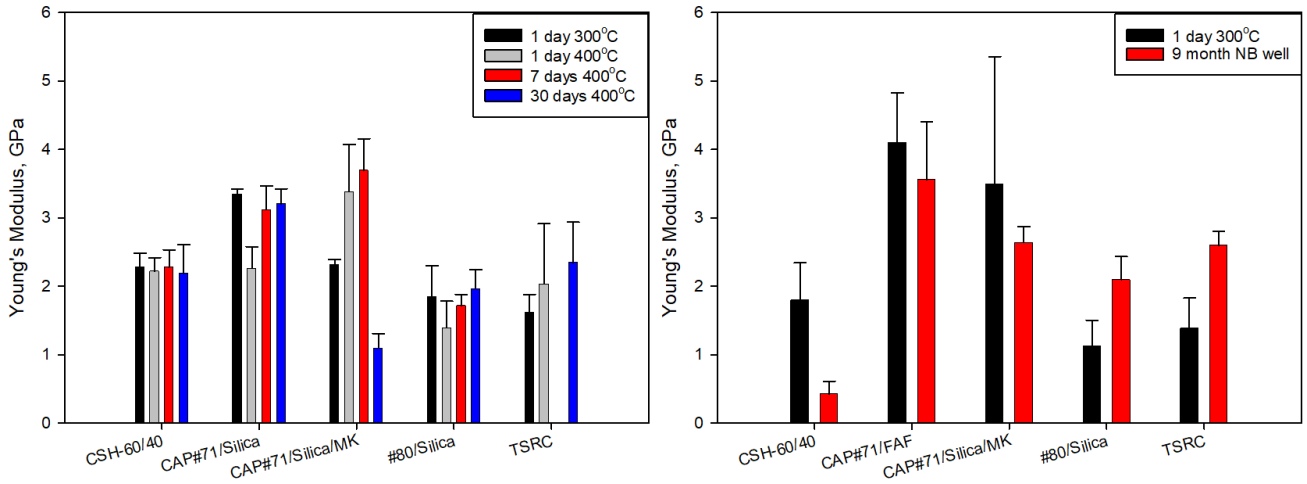

Figure 2: Young's modulus of tested composites after 1-day 300°C autoclaving, supercritical curing, and 9 months of Newberry well exposure.

Another way to evaluate the strength-ductility balance of the cement formulations is to calculate the area under the stress-strain curve, or toughness. The higher toughness allows better chances of survival under the repeated stresses of geothermal wells. The data on the toughness of tested formulations are shown in Figure 3.

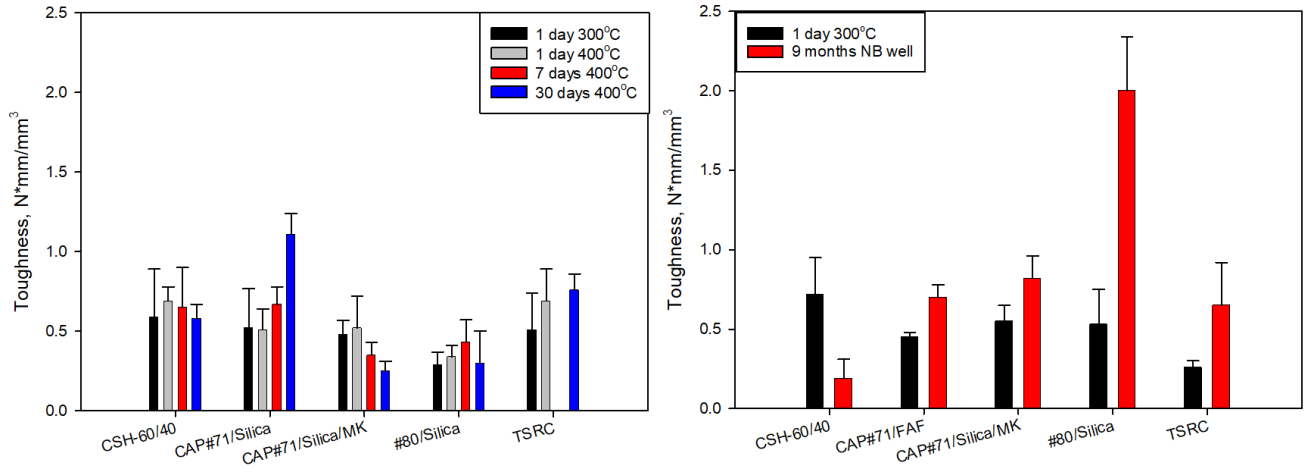

Figure 3: Toughness of tested composites after 1-day 300°C autoclaving, supercritical curing, and 9 months of Newberry well exposure.

For the supercritical samples only OPC-based formulation and CAP cement modified with MK lost some toughness (1.7 and 48% respectively). This was a result of decreased strength and YM for both formulations. For the rest of the formulations, toughness increased, with the increase following the order: CAP#71/FAF (113%) > TSRC (49%) > #80/Silica (3%). The CAP cement toughness increase was due to the strength increase (~9%) and modulus decrease (4%). For TSRC it was the result of the strength increase (59%).

The toughness of all well exposed formulations increased. The only exception was OPC-based formulation that lost most of its strength and modulus resulting in toughness loss of 74%. The toughness increase of #80/Silica formulation was nearly 300%. For the rest of the formulations the toughness increase followed the order: TSRC (150%) > CAP#71/FAF (56%) > CAP#71/Silica/MK (49%).

In summary, most formulations improved their performance through the exposure tests. The trends in properties changes were similar in supercritical and well-exposure tests, except for MK-modified CAP cement. This formulation performed better in the well than under supercritical conditions, where it lost 57% of its strength after the 30-day exposure.

OPC-based HT formulation with silica flour failed strikingly under the geothermal well conditions, losing most of its mechanical properties in the 9-month exposure tests. It also experienced some properties deterioration in supercritical tests.

One of the most important cement functions in geothermal wells is corrosion prevention of steel casing. Casing corrosion is critically accelerated in HT wells. We investigated corrosion protection performance for several formulations under supercritical conditions.

3.2. Ni-alloy/composites lap shear bond strength, bond elongation, and corrosion mitigation by composites after supercritical exposure for 7 and 30 days.

Four of the above formulations were tested with Ni-alloys. These were CSH-60/40, CAP#71/FAF, TSRC, and #80/Silica. The OPC/Silica CSH-60/40 formulation could not be evaluated beyond the exposure due to the adhesive bond failure in the autoclave (Figure 4). The metal plates do not have any cement adhering to them, which shows that this formulation cannot provide any corrosion protection of the metal. The adhesive failure is generally undesirable since it leaves the metal unprotected by the cement coverage.

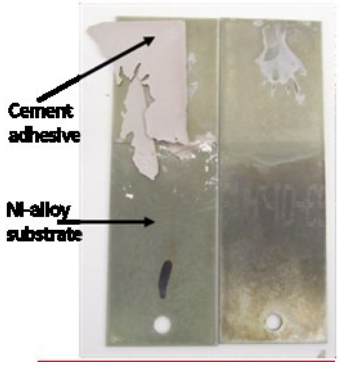

Figure 4: Appearance of the Ni-alloy plates connected by CSH-60/40 at room temperature after 7 days at 400°C.

For the remaining 3 formulations the lap-share bond strength could be tested. The results are shown in Figure 5. The lap-share bond strength decreased in the following order: TSRC > CAP#71/FAF >#80/Silica. For TSRC the strengths of nearly 1.4 MPa and CAP#71/FAF (~1.3 MPa) persisted through 30 days of supercritical exposure. The strength of #80/Silica blend increased by nearly 50% to ~0.9 MPa after 30 days of curing.

Figure 6 shows the appearance of the samples after the lap-share bond tests. Both 7 and 30-day cured TSRC samples failed cohesively in these tests. The plates connected by the composite remain covered with cement layer on both sides, the failure occurred in the cement and not at the interface with the metal. The samples of CAP#71/FAF failed nearly adhesively after the first 7 days but cohesively after 30 days under supercritical conditions. In the adhesive failure one of the plates was covered with the composite while the other remained with very little cement, the bond failed at the interface and not in the cement layer. However, longer curing resulted in the cohesive failure in the cement layer with both metal plates been covered by the binder. The #80/Silica samples failed mostly adhesively at the interface. However, some very thin layer of cement remained on the plates after the 30 days 400°C curing and lap-shear bond testing.

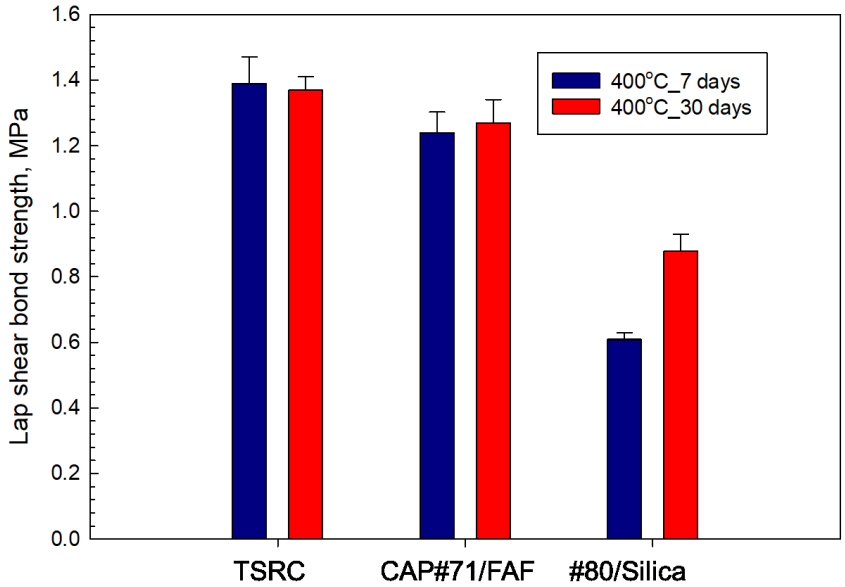

Figure 5: Lap-shear bond strength of cement composites measured after 7 and 30 days of autoclaving at 400°C.

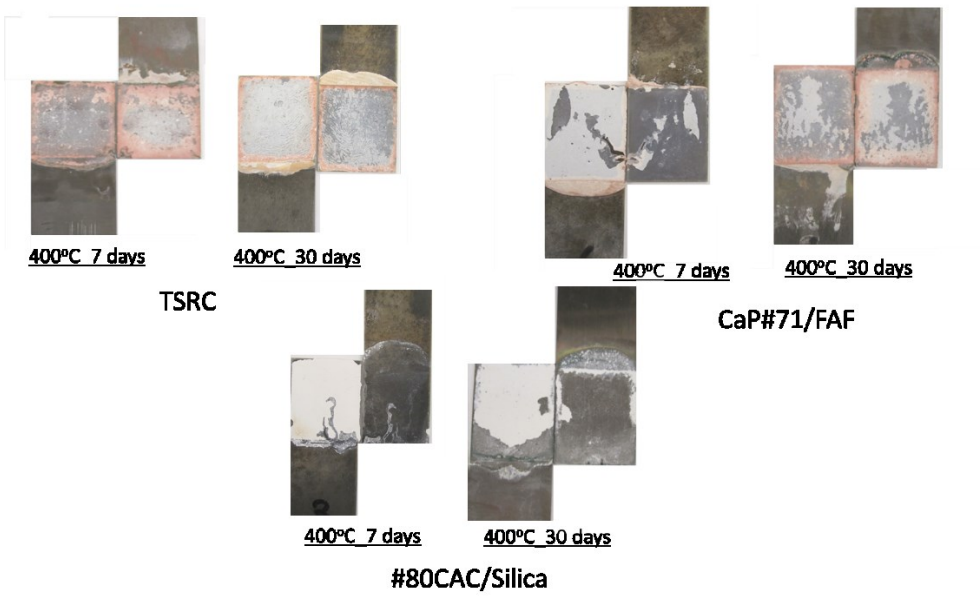

Figure 6: Appearance of the cement composites cured for 7 and 30 days at 400°C after the lap-share bond tests.

Under the conditions of high thermo-mechanical shocks cement-casing bond failure is likely to happen. In the case of cohesive cement failure, the debonded metal will still be protected from corrosion by the adhering cement layer. For the adhesively failed cement the metal will not have any protection after the bond failure.

Another important bond characteristic is tensile displacement before breaking (Figure 7). It shows how much stress the bond can withstand before it breaks. Bond tensile displacement decreased in the same order as the bond strength with TSRC showing the largest displacement of more than 7% before the break and #80/Silica the lowest one of ~3.5% before the break. The percent of bond displacement increased over the curing period for CAP#71/FAF by ~18% along with the improved bond strength and the change of the failure mode from adhesive to cohesive. The bond displacement persisted for TSRC through the 30-day curing.

Figure 8 shows corrosion rates of carbon steel, Ni alloy, and Ni alloy covered with the tested cement formulations as well as the thickness of cement layer on the metal plates after the lap-shear bond tests. The corrosion rates were calculated from Tafel plots measured on the plate with the least coverage and averaged over three locations. As expected, carbon steel had the highest corrosion rate. The corrosion rate of Ni alloy was nearly 2 orders of magnitude lower ($1.48x10^{-1}$ and $1.89x10^{-3}$ mm/year respectively). The corrosion rate dropped by more than 60% with CAP#71/FAF formulation after 7 days under supercritical conditions. It further decreased by an additional 44% after the 30 days of curing down to $4.1x10^{-4}$ mm/year. The corrosion rate of the Ni alloy protected by #80/Silica could be measured only after the 30-day curing. It was double that of CAP#71/FAF formulation and more than 8 times that of TSRC-protected Ni alloy plate. The corrosion rate of the TSRC-protected Ni alloy plate was the lowest – $6.5x10^{-5}$-$1.03x10^{-4}$ after the 7 and 30 days of supercritical conditions respectively. The cement layer was the thickest for CAP#71/FAF composite, its thickness further increased after 30 days. The thickness of the TSRC layer did not change over the test period. The #80/silica blend layer over Ni alloy was the thinnest.

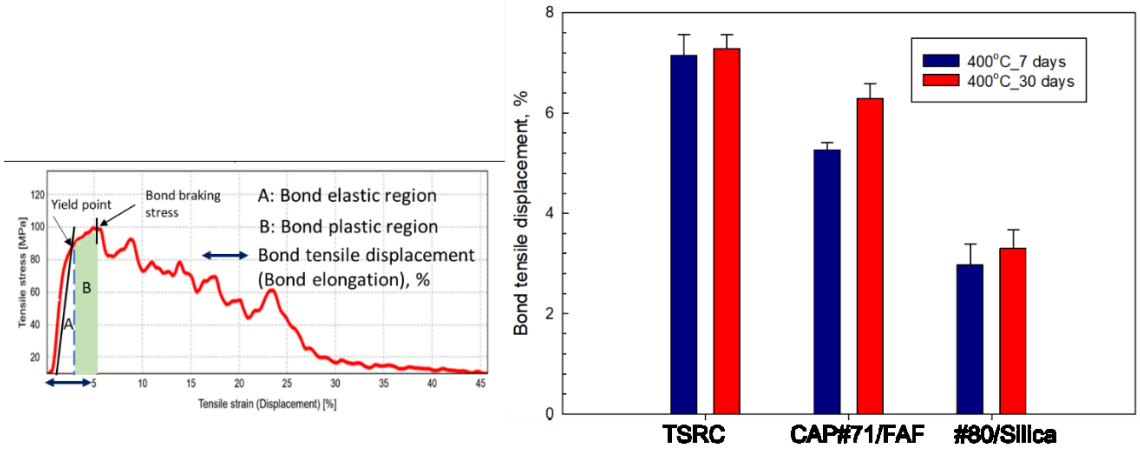

Figure 7: Bond tensile displacement for the cement composites cured for 7 and 30 days at 400°C after the lap-share bond tests.

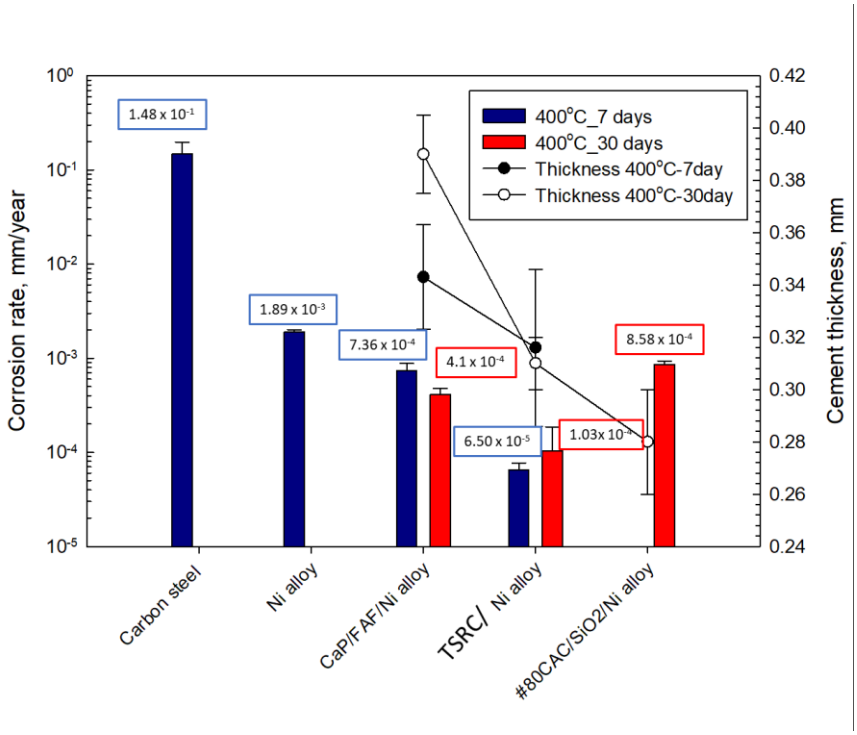

Figure 8: Corrosion rate and cement thickness on Ni alloy after the lap-shear bond tests for samples cured for 7 and 30 days at 400°C.

3.3 Compositions and morphologies of the composites exposed to supercritical and well conditions.

The results of XRD, SEM-EDX, TGA analyses of these and other formulations after the supercritical and well exposure tests were presented in two separate publications (Pyatina et al., 2023; Pyatina & Sugama, 2023b) and are summarized below.

The tests of the mechanical properties of the composites showed that the performance trends of the composites exposed to supercritical conditions for 30 days and to the Newberry well environment for 9 months were comparable. CAP#71-based formulations, TSRC and #80/Silica composites improved mechanical properties during the exposures. Performance of CAP#71 modified with MK and of the control, OPC/silica (CSH-60/40), formulations degraded. Calcium phosphate-based formulations modified with MK experienced some strength lost in well-exposure tests (10%) and significant strength loss in supercritical tests (57%). Since the addition of MK did not improve performance of calcium phosphate composite these samples were not further characterized. For the control, OPC-based formulation the trend reversed: the strength loss in supercritical tests was 13%, in well exposure tests 86%. Properties of the well-exposed OPC-based formulation were not acceptable for geothermal well cementing after the 9 months in the well.

The main difference between the supercritical and well exposures was the exposure environment. In the case of supercritical laboratory tests, it was distilled water and in the well-exposure tests it was CO_2, in its supercritical state. Since the initial phase formation of all the samples started at room temperature (mixing) followed by the 85°C and 300°C hydrothermal curing the phase composition of the tested formulations should be similar for supercritical and well exposure samples, at least to some extent. This was the case for the formulations based on calcium-aluminate cement (calcium phosphate cement, TSRC, and #80/Silica). All of them formed calcium end member of the plagioclase feldspar series anorthite and/or its polymorph dmisteinbergite after the 30-day supercritical curing and the 9-month well exposure. Dioctahedral micas paragonite, muscovite, margarite crystallized only in the 9-month well exposed samples. These phases likely require longer HT curing to crystallize. Boehmite formed in the 30-day supercritical samples was not detected in the well-exposed samples after the 9 months except in the CAP#71/FAF formulation. (It is interesting to note that its presence strikingly decreased after the 9-month exposure when calcium-aluminate cement #71 was replaced with a more Ca-rich cement #50.) All the samples of calcium-aluminate cement-based formulations experienced partial carbonation with formation of calcium carbonate. CO_2 mineralization in crystalline carbonated apatite for calcium phosphate cement samples and cancrinite for TSRC samples was not detected after the 9-month exposure. However, these phases may have formed with low crystallinity that prevented their identification. The extent of carbonation as determined by TGA was on the order of 7-8% for TSRC and CAP#71/FAF samples and less than 2% for #80/Silica samples. Samples morphologies were consistent with their low porosities. Calcium phosphate cement samples showed very dense matrix with inclusions of larger dmisteinbergite crystals and tightly packed micas. Larger calcium carbonate crystals were also detected. Similarly, the dense matrix of TSRC incorporated anorthite and dmisteinbergite crystals with the visible partial conversion of the later into calcium carbonate. The carbonation in calcium-aluminate cement-based blends took place through removal of calcium from plagioclase end-series member anorthite (dmisteinbergite) and formation of the end family member albite (in #80/silica) and mica family minerals margarite, muscovite, and paragonite. These mineral phases allowed persistence or improvement of mechanical properties of the samples during their well

exposure. CMF used in Newberry samples persisted in cementitious composites without any visible degradation improving samples' mechanical properties such as strength and toughness.

For both TSRC and calcium phosphate cement formulations FAF particles were still visible in the matrix after 9 months in the well, suggesting the remaining self-healing capacity of these samples.

The crystalline composition of the CSH-60/40 OPC-based control formulation was dominated by xonotlite after the 30 days under supercritical conditions. Formation of long needle xonotlite crystals resulted in increased samples porosity. The non-reacted silica was still present in the samples after 30 days of curing. The well-exposed samples were completely carbonated: only calcium carbonate peaks were detected by XRD analysis. On the other hand, the SEM/EDX analyses did not show any large calcium carbonate crystals. The matrix was predominately made of calcium bicarbonate with inclusions of large non-reacted silica crystals. The carbonation of the samples proceeded to the formation of a soluble calcium bicarbonate after only 9 months in the well.

The XRD analyses of composites' layers over the metal plates showed that the two major types of minerals in their compositions were those of plagioclase feldspar solid solution series (anorthite, dmisteinbergite, andesine) and mica minerals (paragonite, muscovite, margarite). This was consistent with the bulk compositions of these materials. Some non-reacted phases were also present (grossite in CAP#71/FAF and corundum in TSRC and #80/silica formulations). In TSRC and #80/silica blends made with CAC#80 anorthite was the predominant isomorph of feldspar series endmember, while CAC#71 in CAP#71/FAF formed mostly dmisteinbergite. Bunsenite (NiO) was detected on the Ni-plate covered with CAP#71/FAF, which could be a result of limited or defective coverage. Noticeably, CAP formulation formed mostly muscovite and paragonite mica minerals while TSRC produced Ca-rich and more brittle margarite. The later one crystalizes into big masses that can increase the strength while the former ones are softer and unlikely to increase the strength of the material. This difference can partially be responsible for the strength decrease of CAP cement formulation and its increase for TSRC.

4. CONCLUSIONS

Mechanical properties, including lap-share bond strength with Ni-alloy, and corrosion protection of the alloy by cement composites after exposures for 9 months to conditions of a HT geothermal well (350°C, a CO_2-rich environment) and supercritical laboratory conditions (400°C, water) for 30 days demonstrated that all tested calcium-aluminate-cement-based formulations outperform control OPC/silica blend. The control blend for the most part lost its mechanical properties during the well-exposure (86% of strength loss) with the remaining properties not meeting geothermal well requirements (the residual compressive strength was less than 7MPa). Under the supercritical conditions the blend preserved sufficient mechanical properties however, they deteriorated during the exposure (>13% strength decrease). Bonding strength of this composite with the Ni-alloy could not be measured since the bond broke during the supercritical curing.

All calcium-aluminate-cement-based formulations experienced partial carbonation in the well tests, but their mechanical properties improved throughout the exposure. The carbonation was the smallest for the formulation with the lowest calcium content (#80/silica). Mineralization of CO_2 into crystalline phases was not detected, however, it may have taken place through the formation of nanocrystals and amorphous phases. The crystalline phases formed during the 9-month exposure in the well included plagioclase and mica type minerals expected to be stable under well conditions.

Under supercritical conditions these formulations also improved their mechanical properties. The only exception was calcium phosphate formulation with partial replacement of silica by metakaolin that experienced nearly 57% of strength loss. This formulation was not tested for the bond-strength and corrosion protection of Ni-alloy. TSRC and #80/silica formulations experienced the largest strength improvements of 59 and 42% respectively. The bond strength and corrosion protection of the Ni-alloy increased in the order: #80/Silica < CAP#71/FAF < TSRC. The corrosion rate of Ni-alloy covered with TSRC decreased by ~20 times. TSRC bond failure was cohesive, leaving metal plates covered with cement after the bond-strength tests. The bond failure of #80/Silica formulation was mostly adhesive at the interface and CAP#71/FAF experiences a mixed bond failure- leaving the metal plates mostly covered with the cement layer. CAP#71/FAF composite layer thickness increased after longer curing times, providing further improvement of corrosion protection.

Based on the reported results, calcium-aluminate-cement-based formulations should be used for the cementing of HT and supercritical geothermal wells especially under conditions of CO_2-rich environments where OPC/Silica HT formulation undergoes rapid degradation.

REFERENCES

Asanuma, H., Muraoka, H., Tsuchiya, N., & Ito, H. (2012). The concept of the Japan Beyond-Brittle project (JBBP) to develop EGS reservoirs in ductile zones. *GRC Transactions, Vol 36*.

Asanuma, H., Soma, N., Tsuchiya, N., Kajiwara, T., & Yamada, S. (2015). Concept of development of supercritical geothermal resources in Japan. *International Conference on Geothermal Energy in Taiwan*.

Crow, W., Brian Williams, D., William Carey, J., Celia, M., & Gasda, S. (2009). Wellbore integrity analysis of a natural CO2 producer. *Energy Procedia*, *1*(1), 3561–3569. https://doi.org/10.1016/j.egypro.2009.02.150

Friðleifsson, G., & Elders, W. A. (2005). The Iceland deep drilling project: A search for deep unconventional geothermal resources. *Geothermics*, *34*, 269–285.

Garnier, A., Saint-Marc, J., Laudet, J.-B., Rodot, F., Urbanczyk, C., & Bois, A.-P. (2014). *Carbon Capture and Storage. The Lacq pilot project and injection period 2006-2013. Well Integrity.*

Garrison, G., Uddenberg, M., Petty, S., Watz, J., & Hill, L. B. (2020). Resource Potential of SuperHot Rock. *GRC Transactions, Vol 44*.

Kaldal, G. S., Jonsson, M. T., Palsson, H., & Karlsdottir, S. N. (2015). Structural Analysis of Casings in High Temperature Geothermal Wells in Iceland. *World Geothermal Congress 2015*, *55*(April), 11.

Kuip van der, M. D. C., Benedictus, T., Wildgust, N., & Aiken, T. (2011). High-level integrity assessment of abandoned wells. *Energy Procedia*, *4*, 5320–5326.

Muraoka, H., Asanuma, H., Tsuchiya, N., Ito, T, Mogi, T., & Ito, H. (2014). The Japan Beyond-Brittle project. *Sci. Drill*, *17*(51–59). https://doi.org/10.5194/sd-17-51-2014.

Pyatina, T., & Sugama, T. (2020). Cements with supplementary cementitious materials for high-temperature geothermal wells. *Geothermics*, *86*. https://doi.org/10.1016/j.geothermics.2020.101840

Pyatina, T., & Sugama, T. (2023a). Cements for Supercritical Geothermal Wells at 400oC. *Geothermal Rising Proceedings*, 447–466.

Pyatina, T., & Sugama, T. (2023b). Cements for Supercritical Geothermal Wells at 400oC. *GRC Transactions, Vol. 47*, 447–467.

Pyatina, T., Sugama, T., Garrison, G., Bour, D., & Petty, S. (2023). Results of High-Temperature Cement Blends Exposure in Newberry Well, Oregon. *GRC Transaction, Vo. 47*, 468–488.

Reinsch, T., Dobson, P., Asanuma, H., Huenges, E., Poletto, F., & Sanjuan, B. (2017). Utilizing supercritical geothermal systems: a review of past ventures and ongoing research activities. *Geothermal Energy*, 1–25. https://doi.org/10.1186/s40517-017-0075-y

Sakuma, S., Naganawa, S., Sato, T., Ito, T., & Yoshida, Y. (2021). Evaluation of High-Temperature Well Cement for Supercritical Geothermal Drilling. *GRC Transactions, Vol. 45*, 268–283.

Sminchack, J. R., Moody, M., Theodos, A., Larsen, G., & Gupta, N. (2014). Investigation of wellbore integrity factors in historical oil and gas wells for CO2 geosequestration in the Midwestern U.S. *Energy Procedia*, *63*, 5787–5797.

Sminchak, J., Zeller, E., & Bhattacharya, I. (2014). Analysis of unusual scale build-up in a CO2 injection well for a pilot-scale CO2 storage demonstration project. *Greenhouse Gas Science and Technology*, *4*, 357–365.

Sugama, T., & Pyatina, T. (2022, February 7). Cement Formulations for Super-Critical Geothermal Wells. *47th Workshop on Geothermal Reservoir Engineering*.